Optical third-harmonic generation at interfaces

Thomas Y. F. Tsang
Brookhaven National Laboratory, Upton, New York 11973
(Received 28 April 1995)

Optical third-harmonic generation (THG) is generally a weak process but is dipole allowed, therefore it occurs in all materials, including dielectric materials with inversion symmetry. We report that when using focused high-intensity ultrashort laser pulses, this normally weak THG process becomes highly operative at a simple air-dielectric interface and is much stronger than the bulk of most dielectric materials. We characterized this nonlinear optical response at interfaces as a phenomenological surface-enhanced THG in transmission and/or in reflection. This surface THG is further cascaded in transmission or reflection from layered composite dielectric materials of a high-low index of refraction, resulting in a marked increase in photon conversion efficiency than that of a single interface. Although the present THG efficiency is lower than that of a typical phase-matching harmonic crystal, it is important to note that the surface-enhanced optical THG is a fundamental physical process occurring at all interfaces and is relatively free from the constraint of a phase-matching condition and wavelength restriction. Using optical THG at an interface, it becomes possible to generate wavelengths at which harmonic crystals are unavailable. These findings may lead to a new development of surface-enhanced studies and prompt a reexamination of the processes of high-harmonic generation at interfaces using a focused beam.

PACS number(s): 42.65.Ky, 68.90.+g, 78.66.−w

I. INTRODUCTION

Much is known about the surface second-harmonic generation (SHG) in metals and semiconductors [1]. Numerous applications were based on surface SHG as a powerful and effective diagnostic tool [2]. However, little has been done using third-harmonic generation (THG). It was concluded in a few studies [3] that although the structural symmetry of a centrosymmetric crystal was accurately determined using optical harmonic generation, THG in reflection at metal and semiconductor surfaces is mostly from the bulk, lacking the important surface characteristics. In this paper, we will demonstrate that using femtosecond laser pulses with a fairly simple experimental setup, the normally weak but always electric dipole allowed THG process can be appreciably strong at an ordinary air-dielectric interface and may contain useful surface characteristics. The highly localized THG signal occurring at such interfaces led us to introduce a necessary phenomenological third-order surface nonlinear susceptibility $\chi^{(3)}_{\text{suface}}$, and raised concerns over many previous experiments done on bulk THG in transparent materials.

It is now generally accepted that at an interface, the inversion symmetry of the bulk is necessarily broken. Under the dipole approximation and at wavelengths far from resonance, the broken symmetry at an interface gives rise to an induced nonlinear polarization containing *all* high-order nonlinear susceptibility tensors. In this experiment, using the output beam of a femtosecond laser oscillator focusing on an interface between two different lossless materials, the normally much weaker THG signal is surprisingly strong. Such dramatic enhancement of THG at an interface is believed to be due to a phenomenological surface-enhanced THG, analogous to the well-known surface-enhanced SHG. We demonstrated that such enhancement is highly localized at an interface but not in the bulk. It is conceivable that THG can be enhanced at an interface because the phase-matching condition is less demanding than that in the bulk. We also established that high-order harmonic generation (both even and odd harmonics) at an interface of two different *nonabsorbing dielectric media* using a focused beam is a fundamental physical process and is a universal nonlinear optical property of interfaces. We first reviewed SHG and THG in reflection Si and then presented experimental results on transparent centrosymmetric media; namely, the air-SiO_2 interface and the air-CaF_2 interface, followed by transparent noncentrosymmetric media such as the air-quartz interface and the beta-barium-borate air–BBO interface. We then extended to THG in transmission or reflection on various layer dielectric structures. It is shown that the already strong THG signal from a single interface can be cascaded in layered dielectric structures and is further enhanced in transmission or reflection, such as from the multilayered coatings of a typical laser mirror. Although at present the THG photon conversion efficiency is lower than that of a typical phase-matching harmonic crystal, the THG signal from such dielectric structures is markedly higher than that of a single interface or the corresponding surface SHG. This finding may lead to a development on surface probes using surface THG that can be different from but complementary to surface SHG, and prompt a reexamination of the process of high-harmonic generation at an interface.

Unlike THG in reflection from metals and semiconductors, where the conversion efficiency is often limited by optical damage, the limiting laser intensity irradiating on nonabsorbing dielectric materials is orders of magnitude higher. Although the third-order nonlinear susceptibility $\chi^{(3)}$ of the bulk of a dielectric material is generally smaller than the second-order nonlinear susceptibility $\chi^{(2)}$, the high-order process and the application of a high-intensity laser beam may give a larger induced third-order polarization $\mathbf{P}(3\omega)$ than that of the corresponding second-order polarization $\mathbf{P}(2\omega)$. The situation changes quite dramatically at an inter-

 © 1995 The American Physical Society

face where the discontinuity in the normal component of the electric field gives rise to a large *gradient* in the fundamental electric field normal to the surface, leading to a large nonlinear polarization field. At an interface between two nonabsorbing dielectric media with inversion symmetry, the third-order surface nonlinear susceptibility $\chi^{(3)}_{\text{surface}}$ is always electric dipole allowed while the second-order surface nonlinear susceptibility $\chi^{(2)}_{\text{surface}}$ is allowed only because of the degeneracy lifted by the lack of translation symmetry across the interface, which gives $\chi^{(2)}_{\text{surface}}$ an intrinsically smaller value. This qualitative argument indicates that the induced polarization field $\mathbf{P}(3\omega)=\chi^{(3)}\mathbf{E}^3(\omega)$ can easily exceed that the $\mathbf{P}(2\omega)=\chi^{(2)}\mathbf{E}^2(\omega)$ at an interface. Therefore, with a moderately intense laser fundamental, THG in transmission from dielectric interfaces can be significant.

II. THEORY

For SHG from cubic crystals with inverse symmetry, the second-order nonlinear polarization is given by [2]

$$P_i^{2\omega}=\gamma\nabla_i(\mathbf{E}\cdot\mathbf{E})+\xi E_i\nabla_i E_i, \tag{1}$$

where the first term is isotropic and the last term is anisotropic about the surface normal. Similarly, for THG in centrosymmetric media, the third-order nonlinear polarization is given by [3]

$$P_i^{3\omega}=BE_i(\mathbf{E}\cdot\mathbf{E})+(A-B)E_iE_iE_i, \tag{2}$$

where the first term is isotropic and the second term has anisotropic behavior.

In general, the induced second-harmonic fields have the form [2,4] $E^{2\omega}=a+bf(\theta)$, where a contains a linear combination of isotropic susceptibilities, b contains the anisotropic susceptibilities, and $f(\theta)$ is a combination of sin and cos functions. Specifically, in cubic $\langle 100\rangle$ crystal under a p-polarized excitation, the p-polarized and s-polarized second- and third-harmonic fields are given by [3]

$$E^{2\omega}_{p-p}\propto(\sin^4\theta+\cos^4\theta)-A, \tag{3}$$

$$E^{2\omega}_{p-s}\propto\sin(4\theta), \tag{4}$$

$$E^{3\omega}_{p-p}\propto\frac{A-B}{4}\cos(4\theta)+\frac{3A+B}{4}, \tag{5}$$

$$E^{3\omega}_{p-s}\propto\sin(4\theta), \tag{6}$$

where θ is the azimuthal angle with respect to one of the crystal axes on the sample surface; A and B are constants proportional to the linear optical properties.

In the same manner, the second- and third-harmonic fields generated in cubic $\langle 111\rangle$ crystals are [5]

$$E^{2\omega}_{p-p}\propto A+B(\sin^3\theta-3\sin\theta\cos^2\theta), \tag{7}$$

$$E^{2\omega}_{p-s}\propto(A+B)(\cos^3\theta-3\cos\theta\sin^2\theta), \tag{8}$$

$$E^{3\omega}_{p-p}\propto c\sin(3\theta)+d, \tag{9}$$

$$E^{3\omega}_{p-s}\propto\cos(3\theta), \tag{10}$$

where c and d are additional constants related to the linear optical properties. It can be seen from these equations that cubic $\langle 100\rangle$ and $\langle 111\rangle$ crystals possess fourfold and threefold structural symmetries, respectively. The second- and third-harmonic signals $I(2\omega)$ and $I(3\omega)$ may be expressed as [6]

$$I(2\omega)\propto|\hat{\mathbf{e}}_{2\omega}\bar{\chi}^{(2)}_s:\hat{\mathbf{e}}_\omega\hat{\mathbf{e}}_\omega|^2I^2(\omega), \tag{11}$$

$$I(3\omega)\propto|\hat{\mathbf{e}}_{3\omega}\bar{\chi}^{(3)}_s:\hat{\mathbf{e}}_\omega\hat{\mathbf{e}}_\omega\hat{\mathbf{e}}_\omega|^2I^3(\omega), \tag{12}$$

where $\bar{\chi}^{(2)}_s$ and $\bar{\chi}^{(3)}_s$ are effective surface second-order and third-order susceptibility tensors, respectively, and $\hat{\mathbf{e}}$ is a unit vector.

III. EXPERIMENT

Unlike previous THG experiments [3,6,7] where high-energy pulsed lasers were used, in this experiment, the output intensity 300 mW of average power at the wavelength of 775 nm of a self-mode-locked Ti:sapphire laser oscillator is sufficient to demonstrate the THG in transmission and reflection. The laser was running at a repetition rate of 95 MHz with a pulse duration of 80 fs. To enhance the signal-to-noise ratio, the beam was mechanically chopped at 1 kHz, the harmonic photons were detected by a photomultiplier tube (PMT), and the modulated signal was processed by a standard lock-in technique. Figure 1 shows the detail of the experimental arrangement. All measurements were done in ambient air and the results were reproducible in a vacuum. Linearly polarized laser light was irradiated at a normal angle of incident at the air-dielectric interface of the sample. Using a 10× microscope objective lens for focusing, a maximum peak power density of ~300 GW/cm^2 was achieved in a spot size of $\sim 8\times10^{-8}$ cm^2 with a confocal length of 18 μm. The tight focusing arrangement also allowed the laser beam to spatially select the front or rear interfaces of the samples. The harmonic beams were collimated and dispersed by a quartz prism, and were then detected using a uv-sensitive PMT with appropriate interference filters to block all other scattered photons. A polarizer was placed behind the collimation lens to analyze the polarization content of the harmonic output. The THG nature of the signal was verified by demonstrating its cubic dependence on the intensity of the incident fundamental beam and the correct THG photon wavelength using a monochromator. We noted that THG photons that were generated in the air along the beam path and optics prior to the sample, if any, were filtered out using appropriate bandpass filters before irradiating the sample. And the source of the THG was confirmed to be the sample by the appearance and disappearance of the THG signal when a 1-mm-thick glass slide was placed in front and behind the sample, respectively.

IV. RESULTS

In measurements done on opaque samples, the beam focus was fixed and the specularly reflected harmonics were picked up by a dichroic mirror. For transparent materials, the harmonics were collected in transmission and the samples were scanned along the beam focus so that harmonic photons generated at the front and back interfaces could be measured.

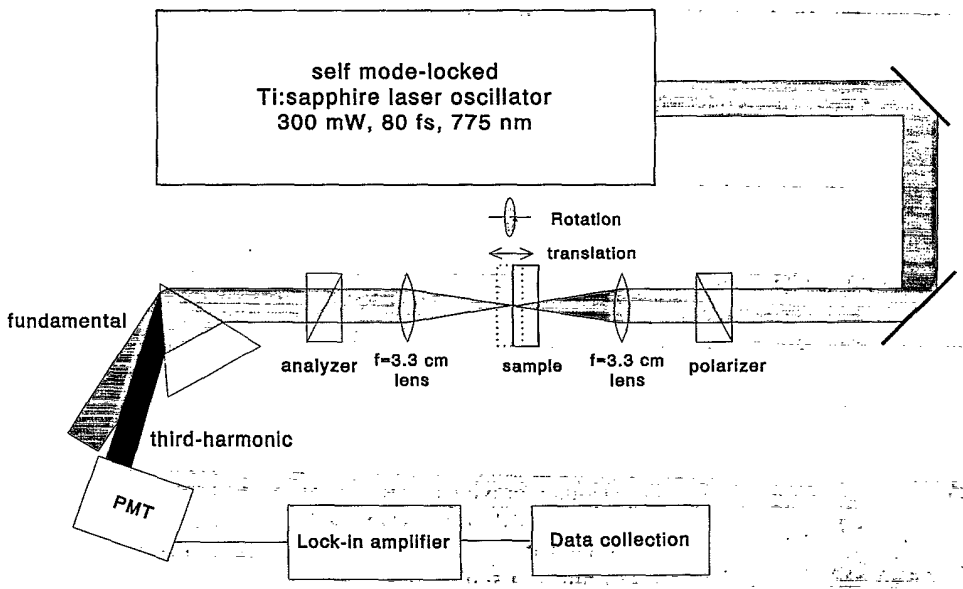

FIG. 1. Experimental arrangement for high-harmonic generation in transmission on transparent materials.

The anisotropic nature of $\chi^{(n)}_{\text{surface}}$ was investigated using a p-polarized fundamental input beam and analyzed in the p-polarized and s-polarized arrangements, p-in p-out and p-in s-out, respectively. Although many isotropic materials and anisotropic materials were tested, we selected only a group of representative materials for this report. In all THG or SHG experiments, the power dependence was checked and verified. Figure 2 illustrates the power-law dependence of 2 and 3 for the normalized SHG and THG signals, respectively, generated at the interface of various samples. Details of each individual sample are discussed below.

A. Centrosymmetric media

1. Crystalline silicon

The anisotropic behavior of SHG in reflection from silicon has been studied extensively [2,3,5]. Here we reproduced some of the SHG results and compared them to the corresponding THG in reflection under identical experimental conditions. Figures 3 and 4 show the anisotropic characteristic of Si⟨100⟩ and Si⟨111⟩ respectively, using different polarization arrangements. Si belongs to a $\bar{4}3$-m point group symmetry class. As predicted in Eqs. (3)–(8) and in Eqs. (5)–(10), Si⟨100⟩ is four-fold degenerate in the p-in p-out arrangement and eight-fold degenerate in p-in s-out on both SHG and THG, giving rise to four and eight intensity peaks

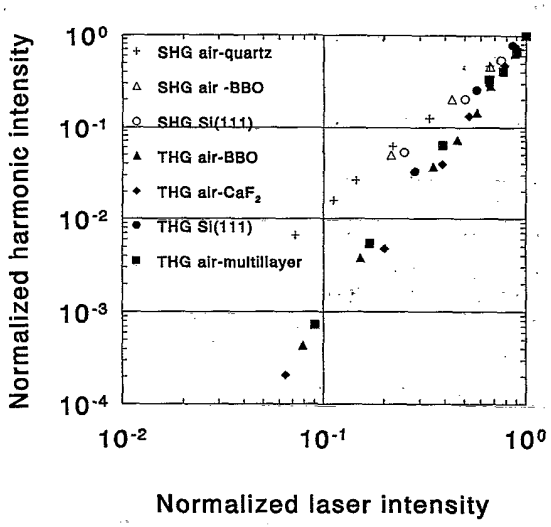

FIG. 2. Normalized logarithmic plot of the harmonic signals generated at the interfaces of several selected materials versus laser intensities.

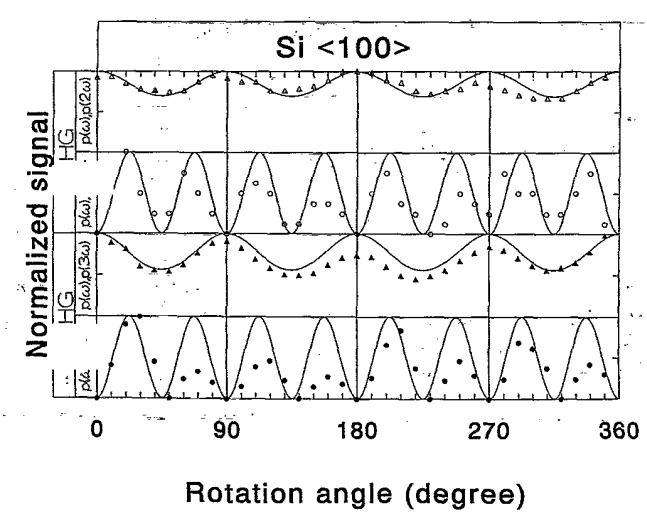

FIG. 3. Rotational anisotropic of the THG and SHG in reflection from a Si⟨100⟩ wafer. The polarization arrangements are labeled in each trace as p-in p-out and p-in s-out. Lines depicted in each trace are the theoretical fitted curves described in the text.

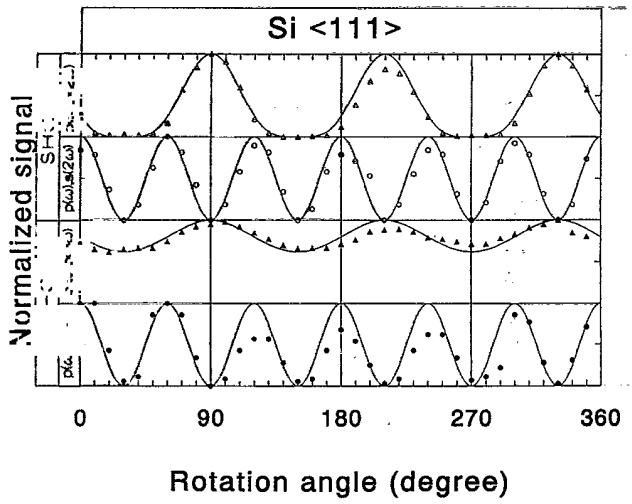

FIG. 4. Same as Fig. 3 but for a Si⟨111⟩ wafer.

under a 360° rotation of the sample about the surface normal. Si⟨111⟩ is three-fold degenerate in the p-in p-out arrangement and six-fold degenerate in p-in s-out on both SHG and THG, giving rise to three and six intensity peaks instead. It is clear that the crystal orientation of Si is resolved by the anisotropic nature of SHG and resolved equally well by the THG technique. However, we noted that the signal strength of the THG is orders of magnitude larger than the corresponding SHG under identical experimental conditions. Figure 5 shows the SHG and THG signals generated in reflection on an Si⟨111⟩ as functions of laser intensities. Since the second-order and third-order processes of SHG and THG, respectively, are well-defined, one can extrapolate the data shown in Fig. 5 to the lower intensities. We then inferred that at the relatively low power density of ~300 MW/cm^2, THG begins to dominate, resulting in a larger number of THG photons than when using SHG. It was suggested that THG is of mostly bulk, having a larger excitation volume than the surface, therefore it is possible that at high

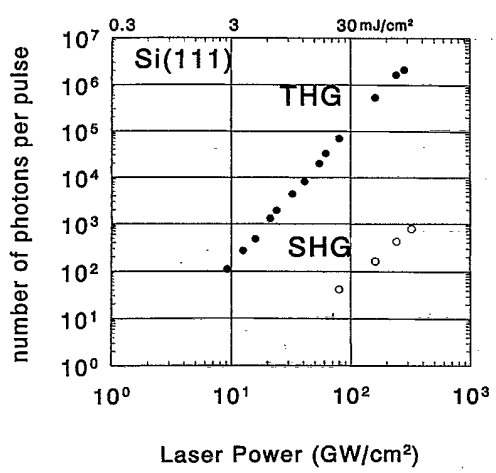

FIG. 5. Power dependence of reflected SHG and THG from Si⟨111⟩.

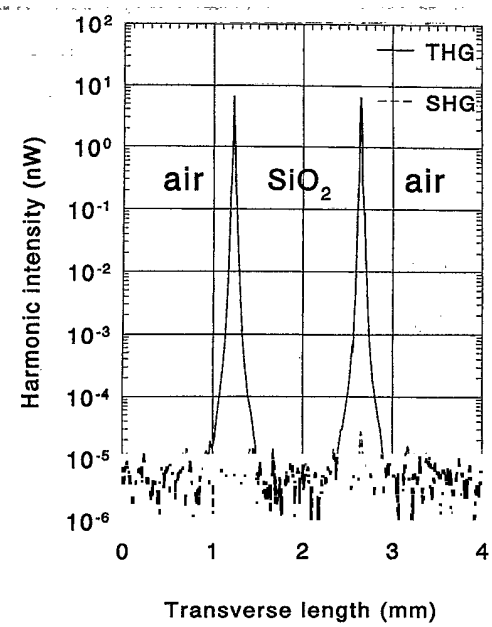

FIG. 6. Second- and third-harmonic (averaged) power generated in transmission at the air-SiO_2 interfaces when a 2-mm-thick fused silica blank was scanned along the beam focus.

intensities harmonic signals are dominated by the THG [3]. However, we speculate that a more effective $\chi^{(3)}_{\text{surface}}$ than $\chi^{(2)}_{\text{surface}}$ may have enhanced the THG process.

The solid lines in Figs. 3 and 4 are normalized theoretical curves predicted by Eqs. (3)–(6) and Eqs. (7)–(10), respectively. For SHG in Si⟨100⟩, the SHG and THG intensities in the p-in s-out arrangements are fitted by Eq. (4) and Eq. (6) but raised to the power of 2. In the p-in p-out arrangements, the SHG signal is fitted by Eq. (3) with $A=-2$. This A value is then used in Eq. (5) to fit the THG data yielding a B value of -1. A similar theoretical fit was performed on the data of Si⟨111⟩ giving its $A \simeq B$, $c=-0.06$, and $d=0.5$. The small ratio of A and B indicated the equal contribution of the isotropic and anisotropic terms, which was also found by other investigators [2,3].

2. *Amorphous fused silica*

A 2-mm-thick optical finish fused silica disk was used. Since fused silica has high transmission at the THG photon wavelength of 258 nm, uv photons generated at the beam focus when it crosses the front and back surfaces of the sample can be collected. With the intensity of the laser beam focused and fixed at a peak power density of ~300 GW/cm^2, the sample was scanned along the beam focus and the SHG and THG photons that were generated in transmission were measured. The absolute intensity of the measured harmonic photons is calculated and plotted after taking into consideration the transmission loss on the interference filters, various attenuators, quantum efficiency of the PMT, and the transmission of the dispersive prism. Figure 6 shows the absolute intensity of THG (solid line) and SHG (dotted line) plotted as a function of the distance traveled. Two strong THG signal peaks were noticeable and were spatially sepa-

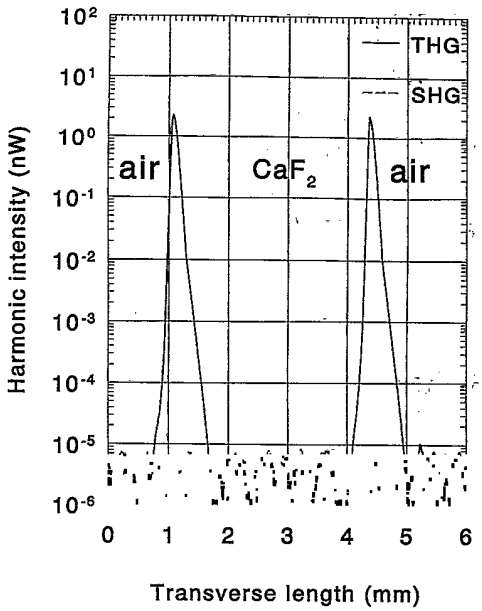

FIG. 7. Same as Fig. 6 but for a 4.77-mm-thick $CaF_2\langle 100\rangle$ disk.

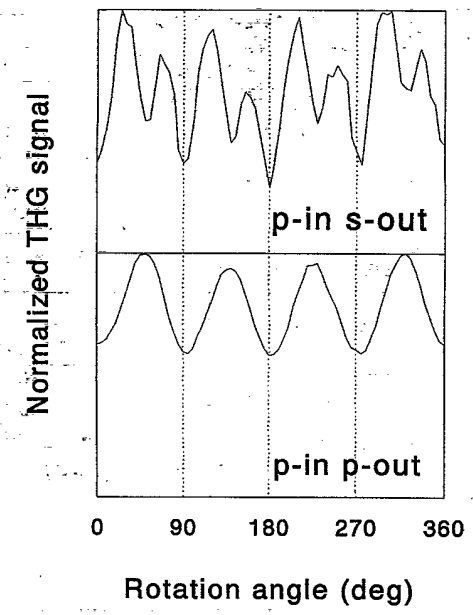

FIG. 8. Anisotropic of the THG signal generated at one of the interfaces of the $CaF_2\langle 100\rangle$ when the same is rotated under the surface normal. Top trace p-in p-out, bottom trace p-in s-out.

rated by ~ 1.45 mm, which is the precise thickness of the fused silica after taking into account its index of refraction and the strong focusing condition from a 10× microscope objective lens. Notice that this apparent reduction in sample thickness also appeared in all other transmission measurements and agrees with the exact sample thickness. It is evident from this data that, at the maximum intensities irradiating the sample, the bulk did not contribute any noticeable THG photon and no measurable SHG photon comes from the interfaces. Since identical laser intensities were launched at the interfaces for SHG and THG measurements and the Fresnel transmission factors are comparable at both wavelengths, based on the data shown in Fig. 6 and the square dependence of $\chi^{(3)}$ on the THG intensity [Eq. (12)], the $\chi^{(3)}_{\text{surface}}$ is at least 3 orders of magnitude larger than the values of $\chi^{(3)}_{\text{bulk}}$ (SiO_2) or $\chi^{(3)}_{\text{bulk}}$ (air). Although the depth of focus of the fundamental beam is only ~ 18 μm far from the angstrom length scale of a molecule to claim any true surface effect, the clarity of the THG signal at the interface suggested that the origin of the THG photons may contain surface characteristics.

3. *Crystalline* CaF_2

Following the same arguments of the previous section, a 4.77-mm-thick CaF_2 (a typical optical window) was also tested. Figure 7 shows THG and SHG signals as functions of the distance scanned. The data is in complete agreement with the SiO_2 results: only THG is evident from the interfaces and none otherwise.

To further examine the versatility of the surface THG, the CaF_2 was tested under azimuthal rotation. CaF_2 is an isotropic material with a cubic crystal structure. This particular sample is cleaved at the $\langle 100\rangle$ plane, therefore it possesses a 4-m structural symmetry under the rotation of the surface normal. Because it is centrosymmetric with no birefringence, under a normal incident angle, the plane of polarization of the fundamental beam remained constant when the sample was rotated about the surface normal. However, closely analogous to surface SHG in reflection from silicon [2] and copper [4], the coupling efficiency between the incident laser source and $\chi^{(n)}_{\text{surface}}$ is dependent on the anisotropy of the surface, the propagation direction, and the polarization of the fundamental light source. At the normal angle of incidence, coupling between the incident fundamental beam and the nth-order surface nonlinearity can occur only through the nonvanishing $\chi^{(n)}$ elements. Therefore, a rotation on the surface normal of the sample would exhibit the crystal symmetry in the high-harmonic generation. We have demonstrated in centrosymmetric media (Figs. 6 and 7) that surface THG is far more easily obtained than the corresponding surface SHG. Figure 8 shows the dramatic symmetry properties of the $CaF_2\langle 100\rangle$ crystal with the p-in p-out and p-in s-out arrangements when the sample was rotated about the surface normal. Under the full 360° rotation, the four-peak and the eight-peak structures were unambiguously revealed, which would be impossible using surface SHG technique under the present experimental conditions. We noted that because of the amorphous nature of the fused silica sample, such rotational anisotropic of surface THG was completely absent. The powerful nature of the surface THG technique, rather than the surface SHG, to unveil the anisotropic characteristic of centrosymmetric transparent crystals on the sample surface is striking.

B. Noncentrosymmetric media

A well phase-matched noncentrosymmetric crystal with a large nonlinear coefficient would generate a sizable amount of second-harmonic photons in the bulk. However, we have shown in the theoretical section that SHG photons can also

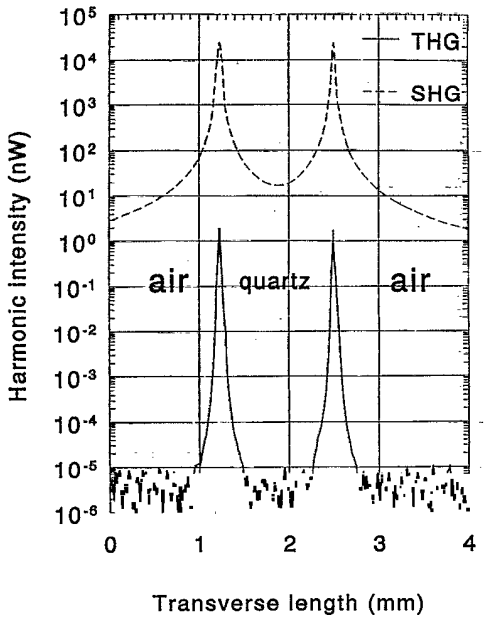

FIG. 9. Same as Fig. 6 but for a 2-mm-thick z-cut quartz disk.

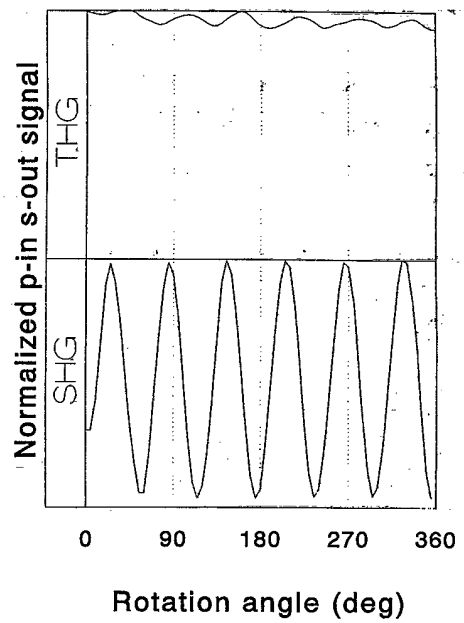

FIG. 10. Anisotropic of the SHG and THG signals generated at one of the interfaces on a z-cut quartz crystal as a function of the azimuthal angles, the polarization arrangements are p-in s-out.

be generated at the interface of any harmonic crystals, and it is a universal property. Since the $\chi^{(2)}_{\text{bulk}}$ is typically $\sim 10^{-9}$ esu while $\chi^{(2)}_{\text{surface}}$ without resonant enhancement is $\sim 10^{-15}$ esu, to observe SHG due only to interfaces but not the bulk on such transparent materials would be difficult, if not impossible, without detuning the crystal away from the phase-matching angle. On the contrary, THG is already difficult to phase match in the bulk but is fairly easy at the interface, as we have shown in the preceding section. Therefore, surface-enhanced THG at an interfaceusing a focused beam, on all centrosymmetric and noncentrosymmetric materials, free from a critical phase-matching condition and a wavelength restriction is interesting at the level of fundamental physics.

1. Crystalline quartz

In this part of the experiment, we used a 2-mm-thick z-cut quartz crystal; that is, the z-axis of the crystal aligned with the surface normal. Once again, the results of SHG and THG in transmission are depicted in Fig. 9, where the phase-matching condition was detuned to a minimum but with the sample surface maintained perpendicular to the irradiating beam path. The harmonic photons due only at the interfaces are clearly seen not only in the THG measurement but also in the SHG measurement. Some bulk contribution to the harmonic signal is observed but only in the broad background of the SHG signal and none in the THG background. It is clear that the surface contribution to the THG is substantial and not negligible, while that of SHG due to an interface is of less importance. It is then no surprise to see two small SHG signals, and also, of course, two strong THG signals, temporally separated precisely by the thickness of the harmonic crystal, copropagating with the harmonic signals due to the bulk, during any routine frequency double or triple that of a fundamental beam using a focused beam. In fact, most experimenters working with intense ultrashort laser beams have been disregarding these small harmonic signal contents and categorized them as spikes or reflection from elsewhere. One might think that placing antireflection coatings on all high-power optics would prevent such high-order surface phenomena. But as we will discuss in the last section, antireflection coatings are quite subtle. It would, on the contrary, produce unanticipated negative effects.

Under the present experimental arrangement, the z-cut quartz is optically inactive; that is, the polarization of the fundamental beam is invariant along the z axis of the crystal. Coupling between the incident fundamental beam and the nth-order surface or bulk nonlinearity can occur through the nonvanishing $\chi^{(n)}$ elements, and a rotation on the surface normal of the sample would exhibit the crystal symmetry by measuring the high-harmonic intensities either in the bulk or at the surface. Figure 10 shows only the salient features of the measurement, where the harmonic signals are measured at an interface with a p-in s-out arrangement. The anisotropic nature of the z-cut quartz is evident. Under the full 360° azimuth rotation, a 3-m point group symmetry is revealed by six highly modulated SHG intensity peaks, and six weakly modulated THG intensity peaks.

2. Beta-barium-borate (BBO) crystal

A 1-mm-thick BBO cut at 31° intended for efficient frequency double that of a Ti:sapphire laser is employed. It is not disputed that a properly phase-matched BBO crystal generates large SHG and THG in the bulk [8], and the birefringence is substantially larger than that of the quartz. BBO is a highly optical active material and is sensitive to depolarization effects, and the polarization of the fundamental beam varies under the rotation of the azimuth. Although BBO belongs to a trigonal system with a point symmetry of 3 m, harmonic generation becomes rather complex because of the nonvanishing $\chi^{(n)}$ elements coupled to the local polarization.

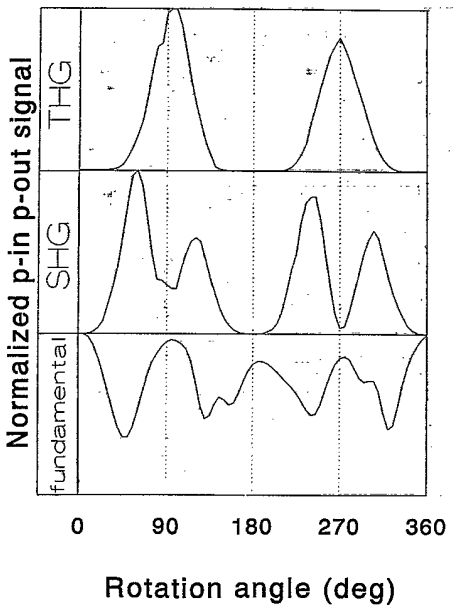

FIG. 11. Anisotropic of the fundamental, SHG, and the THG signals generated at one of the interfaces on a BBO crystal as a function of the azimuthal angles; the polarization arrangements are p-in p-out.

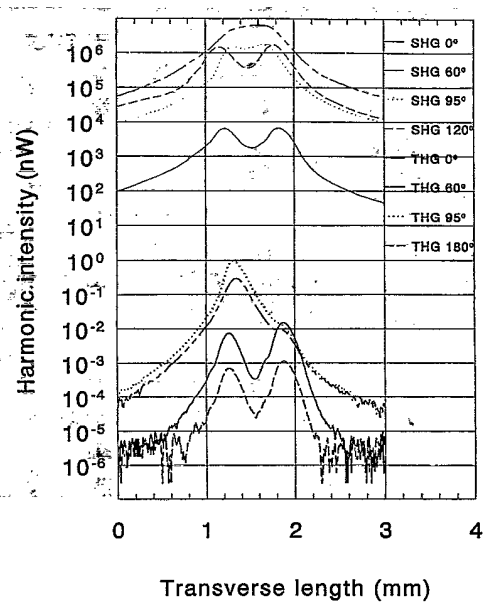

FIG. 12. Same as Fig. 6 but for a 1-mm-thick BBO crystal at various azimuth angles, and the focusing condition is relaxed using a lens of 3.3-cm focal length.

Figure 11 shows the anisotropic behavior of the present BBO crystal at one of the interfaces in the azimuthal rotation under the p-in p-out arrangement. The normalized intensities of the fundamental, SHG and THG are depicted. It is interesting to note that even for a popular BBO crystal, SHG and THG are observed at the interfaces; however, no attempt is made here to provide detailed analysis on the already well-documented crystal orientation [9] using this surface-enhanced nonlinear phenomenon. Also, the possibility of THG through sum frequency generation between the fundamental and the SHG beams may have significantly changed the measured symmetry properties using THG at the BBO interface. Figure 12 gives the SHG and THG signals generated when the BBO crystal is scanned across the focus plane at various azimuthal angles (see Fig. 11 for details). Because of the tight focusing and the high repetition rate of the experimental arrangement, in order to avoid thermally detuning the crystal and to prevent optical damage due to accumulative effects, a 3.3-cm focusing lens instead of a 10× microscopic objective lens is used in this part of the experiment. As a result, the spatial width of the harmonic signals generated at each interface is not as sharp as data presented earlier. Nevertheless, SHG and THG signals, due only to the interfaces, are unambiguous at the unfavorable azimuthal angles where efficient phase matching is mostly suppressed: at 0°, 120°, and 180°. Dominance of the bulk over the surface contribution in the harmonic signals is evident at the otherwise favorable azimuthal angles of 60° for the SHG and 90° for the THG. The gradual shifting of the importance of the bulk to surface under the rotation of the azimuthal angle is clear. We noted that the conversion efficiency of the THG is lower than that of Ref. [8] due to the strong focusing condition necessary to spatially probe the interfaces with confocal lengths much less than the crystal thickness.

C. Layered dielectric structures

Since the majority of the THG signal is coming from an interface, placing antireflection dielectric coatings on a surface may eliminate this nonlinear phenomena. Yet we will show in the following examples that negative and totally unanticipated effects resulted [10]. We first have to realize that surface THG is probably due to the presence of a field *gradient* across an interface. A composite of layered high-low index of a dielectric structure would naturally create more interfaces, thus more potential THG sources. Therefore, the measured THG signals is expected to increase linearly with the number of THG production sites; that is, the total number of interfaces provided that the materials are transparent both at the fundamental and the THG wavelengths. We illustrated this cascade THG process with two examples and then discussed their consequence. We noted that in order to provide a long interaction length for coherent excitation, experiments described in this section were conducted with a longer confocal length by focusing the fundamental using a 3.3-cm focusing lens instead of a microscopic objective.

1. Two-layered system

A simple two-layered system can be easily constructed by placing two fused silica together with an air spacer. Two 2-mm-thick optically flat silica windows were pressed together with a sheet of ~40-μm-thick mica ring, leaving an air spacer in between. Figure 13(b) shows the details of the construction. The pulse duration of the laser is ~100 fs, which gives a coherent length of ~30 μm in air and is comparable to the thickness of the air spacer. Also, the confocal parameter of the laser focused by a 3.3-cm lens is ~120 μm, which is much larger than the thickness of the air spacer. Therefore, coherent THG excitation at the interfaces

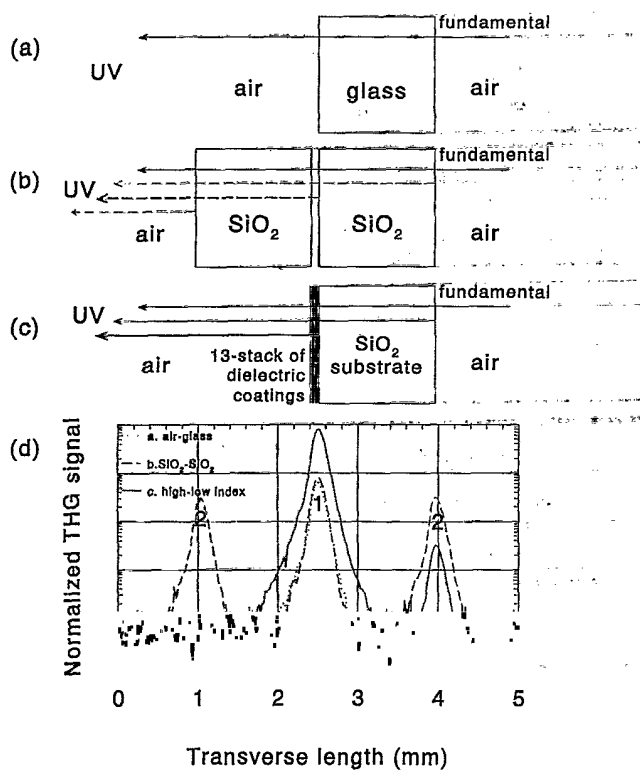

FIG. 13. (a) Schematic of THG at an air-glass interface; only uv photons generated at one interface are propagated and measured. (b) Same as (a) but for a SiO_2-air-SiO_2 two-layered structure and with a 40-μm spacer in between. uv protons are propagated and measured on all interfaces. (c) Same as (a) but for a SiO_2 substrate with a stack of layered high-low index dielectric structures. uv photons are propagated and measured on both interfaces. (d) logarithmic plot of the measured THG signals for the arrangements of (a), (b), and (c) versus the distance scanned by the samples along the beam focus.

and propagation of the uv protons from the SiO_2-air-SiO_2 spacer is possible. Three strongly localized THG signals are evident when the fundamental beam is selectively focused onto the interfaces of this SiO_2-air-SiO_2 structure [dashed line of Fig. 13(d)]. The THG signal originating from the SiO_2-air-SiO_2 spacer [label No. 1 in Fig. 13(d)] is approximately twice as strong as those from the two SiO_2-air interfaces [label No. 2 in Fig. 13(d)]. We noted that the y-scale of Fig. 13(d) is logarithmic. For comparison purposes, the THG from the surface of a microscopic glass slide under identical experimental conditions is also depicted in Fig. 13(a) and the results are plotted as doted lines in Fig. 13(d). Only a single signal peak is observed in the forward direction at the glass-air interface because the glass prohibited the propagating of the uv photons generated at the other air-glass interface. We noted that the refractive index of glass is larger than that of the fused silica, and the transmission at the fundamental wavelength is comparable in glass and fused silica. We further speculated that the larger uv signal from glass is due mostly to a larger field gradient across the interface. More examples of this argument will be given in the discussion.

A couple of observations can be made from these results. First, the surface THG signal can be cascaded. Second, material that can support a larger field gradient at an interface, that is, larger refractive index, produces more THG photons. Therefore, a traditional multilayered dielectric thin film that has a high-low index of refraction would accidentally act as a unique THG source.

2. *Multiple-layered system*

As a preliminary test of the above mentioned hypothesis, a multilayered dielectric mirror was selected, but not constructed, from the available mirrors in our laboratory. A typical uv (266-nm) reflector was used. The composition and structure of the layered dielectric mirror were analyzed using an x-ray diffraction technique. It consisted of ~13 stacks of high-low index structures made of HfO_2 (~310 Å thick) and SiO_2 (~440 Å thick) of the reflecting surface, with a total physical thickness of ~1 μm [see Fig. 13(c) for details]. Sine both materials are transparent at the THG wavelength of 258 nm and the fundamental wavelength of 775 nm, and the thickness of the stacks is much less than the coherent length of the laser or the confocal parameter, coherent THG at all interfaces with maximum strength is possible. Because the present dielectric mirror is a uv 266-nm high reflector, it is therefore constructed at the thickness of $\lambda/4\eta$, where η is the index of refraction of HfO_2 ($\eta=2.1$) or SiO_2 ($\eta=1.5$) at the THG wavelength of 258 nm. However, when the fundamental beam is focused on this dielectric stack, THG at every interface is either transmitted or reflected. Therefore, ~50% of the accumulated THG photons that are generated at all interfaces are expected to propagate in the forward direction and can be measured, and the remaining THG photons are reflected. We measured, in the forward direction, the cascaded THG photons to be more than ten times higher [see the solid line in Fig. 13(d)], than that of the single interfaces or the two-layered structure described in this paper. Two THG signals are actually seen in Fig. 13(d); a much stronger signal originated from the multilayered dielectric structure and a weaker signal from the back surface of the substrate. We believe that the large field gradient across the HfO_2-SiO_2 interfaces and the cascade process occurred at all 13 layers of high-low index materials have contributed to the high THG photon yield.

Although the thickness and the number of dielectric stacks are not optimal, the fact that it produced a sizable amount of THG photons (an absolute a value will be given in the next section) at the interfaces of its layered dielectric structure is striking. It is conceivable that such surface THG from a carefully designed dielectric composite will give orders of magnitude more THG photons. Experiments targeted toward this direction are in progress.

V. DISCUSSION

The significance of this study suggests that using a focused beam THG at an air-dielectric interface is much stronger than the bulk of most dielectric materials, particularly in noncentrosymmetric media. This nonlinear phenomenon may have been overlooked in the past. Some of the previously measured $\chi^{(3)}_{\text{bulk}}$ values may have been dominated by the $\chi^{(3)}_{\text{surface}}$. For a direct comparison of the $\chi^{(3)}_{\text{surface}}$ measured in this experiment to the literature value of $\chi^{(3)}$ of air, we measured the THG photon yield in air and at the interface of a

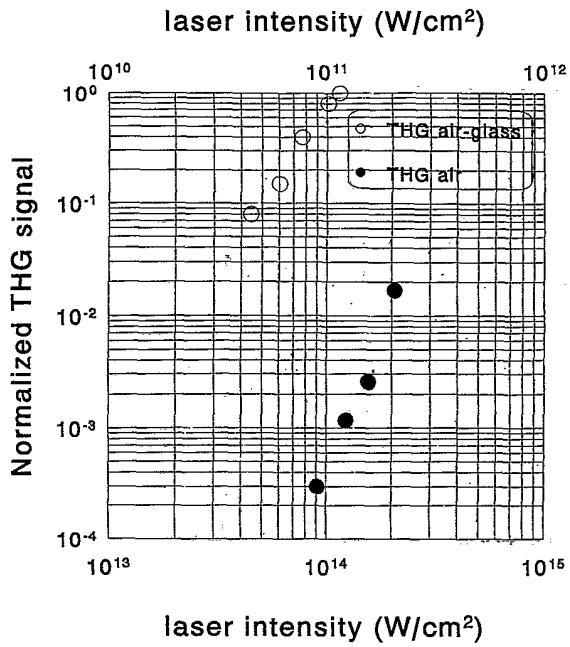

FIG. 14. Direct comparison of THG in air and at an air-glass interface, hence a direct comparison on the $\chi^{(3)}$ values. Bottom x axis is for the data of THG in air and the top x axis is for the THG at the air-glass interface. Measurements are done using a kHz regenerative amplified Ti:sapphire laser instead.

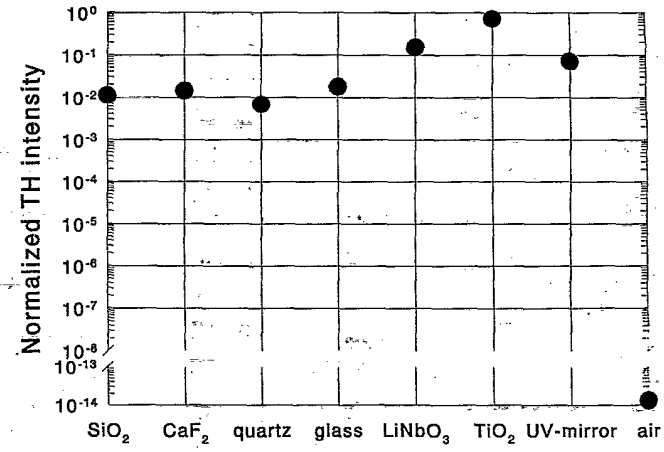

FIG. 15. Comparison on the surface THG yield in transmission for various dielectric materials. At a maximum input laser fluence of 300 GW/cm^2, the maximum y scale ($y=1$) corresponds to a conversion efficiency of 10^{-7}. One of the x labels uv mirror, is the multilayered dielectric mirror described is the text.

1-mm-thick glass slide under identical experimental conditions. In order to collect measurable THG photons generated in air, the output energy of the Ti:sapphire laser oscillator is amplified in a kHz regenerative amplifier. Precautions were taken to avoid a white light continuum generation, but only THG occurred when working with the glass slide. The results are plotted in Fig. 14 with a different x axis for each material. The top x axis displays a lower intensity for the glass, whereas the bottom x axis shows a higher intensity for air. By extrapolating this data, the THG yield at the air-glass interface is larger than that of air by $\sim 10^{12}$. Given that the THG intensity is proportional to the square of $\chi^{(3)}$[see Eq. (12)], and both measurements are third-order processes, the $\chi^{(3)}_{\text{surface}}$ at the air-glass interface is then $\sim 10^6$ larger than the corresponding value of air. Taking the reference $\chi^{(3)}$ value of air to be $\sim 10^{-17}$ esu [11], the inferred $\chi^{(3)}_{\text{surface}}$ of an air-glass interface would be 10^{-11} esu, which agrees reasonably well with the measured value of 1.86×10^{-11} esu in this experiment. However, the noticeable difference is that our measured value is entirely due to the air-glass interface but not the bulk. Similarly, our measured $\chi^{(3)}_{\text{surface}}$ values for fused silica and TiO_2 are $\sim 10^{-11}$ and $\sim 10^{-10}$ esu, respectively (see Fig. 15). We also noted that this nonlinear optical response at interfaces can in fact be characterized as a phenomenological odd-harmonic generation process, where fifth-harmonic generation was also observed under identical experimental conditions but with a significantly lower signal level. Details of this investigation will be presented elsewhere.

We hypothesize that THG enhancement at an interface is due to the existence of a third-order surface nonlinear susceptibility $\chi^{(3)}_{\text{surface}}$ which may have been enhanced by a tight-focusing condition. The nonlinear interaction with focused Gaussian beams has been discussed by Boyd [11]. Because there is a π radian phase shift that occurred on the fundamental beam when passing through its focus and a three times larger phase shift experienced by the third-order nonlinear polarization, a nonzero positive wave vector mismatch introduced in a tight-focusing condition can be used to compensate for such a phase shift experienced by the surface nonlinear polarization. The consequence of this tight-focusing condition might provide an explanation for the high THG efficiency at an interface. We also have indications that the strength of $\chi^{(3)}_{\text{surface}}$ may be a function of the field gradient. TiO_2 and $LiNbO_3$ have a significantly larger index of refraction than fused silica or glass, hence, it conceivably can provide a larger field gradient at their interfaces. The normalized THG intensity of these dielectric materials is plotted in Fig. 15. Indeed, the result suggests that higher index materials give better THG conversion efficiency. However, as shown in Fig. 15, the multilayered dielectric mirror has a lower THG yield than a high-index substrate. But the difference in the refractive index of HfO_2 and SiO_2 at the fundamental wavelength of 775 nm is 0.5, while that of the $LiNbO_3$ or TiO_2 and air is ~ 1.6. The smaller difference found in the present multilayered dielectric stack and the high-order effect of the THG may favor a single interface of higher index materials in some specific cases. Therefore, a single interface of high-index material will in some cases give a larger THG photon conversion efficiency than a multilayered dielectric stack. Clearly, more studies are needed to establish a precise relationship between the $\chi^{(3)}_{\text{surface}}$ and the field gradient. Although a typical bulk THG phase-matching length of these materials is a few macrons ($l_{\text{eff}} \simeq \lambda/\{4[\eta(\omega)-\eta(3\omega)]\}$) and is longer than the total thickness of the dielectric stack of ~ 1 μm, we noted, however, that phase matching at an interface is noticeably different than the bulk and is a challenging issue. At the maximum power density of ~ 300 GW/cm^2 used in most of this experiment, an absolute THG

photon conversion efficiency of 10^{-7} was found at the interface of TiO_2.

VI. CONCLUSIONS

There are many contributions to this work. We established that a simple interface between two different nonabsorbing dielectric media is a source of second- and third-harmonic generation. Because the symmetry at an interface between two different centrosymmetric media is necessarily broken in the normal direction, a large field gradient exists. Such a large field gradient dramatically enhances the THG process at an interface in centrosymmetric or noncentrosymmetric materials. The enhancement of the THG at an interface may greatly expand the capability of using THG as a diagnostic tool in the study of interfaces. More importantly, the mechanism behind the origin of harmonic generations at dielectric interfaces of transparent materials using a focused beam is of scientific interest. Since large THG was observed at the interface rather than the bulk of most materials, it raises concerns over many literature values of $\chi^{(3)}$ where experiments were mostly conducted using materials thinner that the confocal length of a laser, and the distinction between the contribution from the surface and the bulk were lost.

Using the surface THG technique, rather than the more difficult SHG, to resolve the structural symmetry of a centrosymmetric dielectric crystal is unprecedented. Surface-enhanced THG at interfaces of any media free from the constraint of a phase-matching condition and wavelength restriction is striking. The technique of optical THG at an interface may open up a new direction to generate wavelengths in which harmonic crystals are unavailable. Cascading many layers of nonabsorbing high-low index of refraction dielectric media to form multiple interfaces can largely enhance the THG signal. The results have practical implications when an optimal dielectric composite gives adequate photon conversion efficiency.

ACKNOWLEDGMENTS

I acknowledge the support of Veljko Radeka. I thank John Warren for the x-ray structural analysis and appreciate the technical assistance of John Schill and Kathy Warburton. This manuscript has been authored under Contract No. DE-AC02-76CH0016 from the U.S. Department of Energy.

[1] Y. R. Shen, *The Principles of Nonlinear Optics* (Wiley, New York, 1984).
[2] Y. R. Shen, Nature **337**, 519 (1989); H. W. Tom, T. F. Heinz, and Y. R. Shen, Phys. Rev. Lett. **51**, 1983 (1983).
[3] D. J. Moss, H. M. van Driel, and J. E. Sipe, Appl. Phys. Lett. **48**, 1150 (1986); J. E. Sipe, D. J. Moss, and H. M. van Driel, Phys. Rev. B **35**, 1129 (1987).
[4] H. K. Tom and G. D. Aumiller, Phys. Rev. B **33**, 8818 (1986).
[5] G. Lüpke, D. J. Bottomley, and H. M. van Driel, J. Opt. Soc. Am. B **11**, 33 (1994); D. J. Bottomely, G. Lüpke, J. G. Mihaychuk, and H. M. van Driel, J. Appl. Phys. **74**, 6072 (1993).
[6] G. Berkovic, R. Superfine, P. Guyot-Sionnest, and Y. R. Shen, J. Opt. Soc. Am. B **5**, 668 (1988).
[7] P. D. Maker and R. W. Terhune, Phys. Rev. **137**, A801 (1965).
[8] R. C. Eckard, H. Masuda, Y. X. Fan, and R. L. Byer, IEEE J. Quantum Electron. **26**, 922 (1990); I. V. Tomov, B. Van Wonterghem, and P. M. Rentzepis, Appl. Opt. **31**, 4172 (1992).
[9] D. N. Nikogosyan, Appl. Phys. A **52**, 359 (1991).
[10] T. Tsang, Appl. Opt. **33**, 7720 (1994).
[11] Robert W. Boyd, *Nonlinear Optics* (Academic, New York, 1992), p. 163.